Solvent-mediated pathways to gelation and phase separation in suspensions of grafted nanoparticles

Manos Anyfantakis,[ab] Athanasios Bourlinos,[c] Dimitris Vlassopoulos,*[ad] George Fytas,[ad] Emmanuel Giannelis[c] and Sanat K. Kumar[e]

Received 8th June 2009, Accepted 30th July 2009
First published as an Advance Article on the web 27th August 2009
DOI: 10.1039/b911244h

We explore the role of the solvent medium on the interplay between gelation and phase separation in suspensions of organosilicate planar hybrids grafted with hydrocarbon chains. We establish their phase diagram by means of dynamic light scattering, rheology and visual observations, and different routes to gelation, depending on the solvent used. In agreement with earlier works, the solvent quality for the grafted chains at a given temperature controls the balance between attractions and repulsions, and hence the phase diagram of the nanoparticles and their tendency to gel. Here we show how to tune the suspension state and hence its rheology. For decane, a good solvent for the hydrocarbon chains, gelation occurs at rather low volume fractions in the presence of phase separation. This is due to the interdigitation of solvent molecules with the grafted chains, resulting in their crystalline packing that promotes the attraction between particles. For toluene, a solvent of reduced quality for the hydrocarbon chains, no interdigitation takes place, and hence gelation is triggered by clustering at higher volume fractions before phase separation. Our results support the generic picture of complex kinetic arrest/phase separation interplay in soft matter, where phase separation can proceed, be interrupted or be completely inhibited. A number of interesting possibilities for tailoring the rheology of grafted colloidal systems emerge.

I. Introduction

The study of colloidal suspensions ranging from the dilute (gas) to glassy regimes has been in the forefront of soft matter research for many years due to the related fascinating scientific challenges and technological applications.[1–3] Typically, the interplay between flow field and spatial organization has important implications in areas ranging from rheology control to nanocomposites and reinforced polymers.[4–7] Size, shape and interparticle potential are key particle properties which dictate, in as yet not fully predictable manner, the rich phase behavior, the thermorheological properties and the formation of non-equilibrium, dynamically arrested glass or gel states of the colloidal systems.[8–13] These poorly understood states of matter occur in diverse systems which extend well beyond the conventional spherical colloids, *e.g.*, biopolymers, associating polymers, clays, polymer nanocomposites and emulsions, exhibiting a rich interplay between repulsive and attractive interactions.[14,15] As a general rule, geometrical percolation due to clustering and/or enhanced density fluctuations due to a thermodynamic phase transition can lead to topological constraints and arrested states.[16–18]

Despite the significant progress made to date, a thorough understanding of the origins and mechanisms of dynamic arrest is still missing. In some cases, progress has been slow even at the phenomenological level. For example, despite their importance, anisotropic particles have received much less attention compared to their spherical counterparts. Yet, it is clear that shape leads to quantitatively and, sometimes, qualitatively different behavior.[19–21] For instance, for the widely studied case of hard-sphere colloids, the glassy phase (repulsion-dominated) is formed for volume fractions $\phi > 0.5$ as a result of excluded volume interactions and strong dynamic cooperativity in the absence of a macroscopic phase separation;[1,2,22] in the same systems, gelation (attraction dominated) takes place at low volume fractions ($\phi \sim 0.2$) but only under the influence of osmotic force of added depletants.[9,12,22,23] In contrast, in clay suspensions (which are typical anisotropic systems), like laponite consisting of charged colloidal discs, dynamic frustration occurs at relatively low $\phi \ll 0.5$, implying a large effective pervaded volume without necessarily the involvement of a phase separation;[18,19,23–27] this is analogous to the differences between polymeric flexible coils and rods.[28] Note that gelation is much more common in these anisotropic systems than glass transition (at high volume fractions orientational order and/or phase separation may well take place).[29] Alternatively, in polymer nanocomposites the vicinity of phase coexistence between a polymer-rich and a clay-rich phase might play a role in the solidification of the system.[30] Such solidification phenomenon in diverse materials should have a generic origin and features; this calls for more experiments with different particles of varying shape and controlled interactions. However, a frequent experimental concern is the fact that

[a]*Institute of Electronic Structure & Laser, FORTH, Heraklion, Crete, Greece*
[b]*Department of Chemistry, University of Crete, Heraklion, Crete, Greece*
[c]*Department of Materials Science and Engineering, Cornell University, Ithaca, NY, USA*
[d]*Department of Materials Science & Technology, University of Crete, Heraklion, Crete, Greece*
[e]*Department of Chemical Engineering, Columbia University, New York, NY, USA*

anisotropic particles are usually ill-defined (*e.g.*, the industrial laponites or montmorillonites) and the obtained structure and dynamics results are often not reproducible or contradictory, apparently because of different interactions, additives present or sample treatment. It is thus highly desirable to establish protocols for handling such systems in a way that allows unambiguous comparison of experimental findings, or obtain true model anisotropic colloidal particles for studies of phase state and dynamic behavior. In recent years, the latter has indeed emerged as an important field of research, and in fact some efforts in this direction have already materialized.[31–35]

An additional issue of substance is the need to gain more insight into phase transitions that may occur *via* surface modification in a variety of colloidal particles. This intimately relates to the problem of colloidal stabilization. It is well-known that the macroscopic phase of a given colloidal dispersion reflects the balance between attractions (at large separations) and repulsions (at short distances). Typically, in an electrically neutral suspension, grafting of the particles provides a screening of the van der Waals attractions, resisting flocculation.[36,37] It turns out however, that the details of the surface modification (*e.g.* grafting procedure, nature of grafted chains and their interactions with the suspending medium) play a central role in the behavior of the suspension.[38] For example, dispersions of silica particles stabilized by means of grafted alkyl chains in organic solvents are known to form thermoreversible gels, but the origin of the gel state has been linked to different mechanisms (percolation, solvent-mediated interactions, dynamic instability or frustrated gas–solid transition).[39–44] Therefore, the detailed understanding of surface modifications in colloidal systems holds the key for understanding and hence manipulating colloidal interactions and transitions.

In this work, we attempt at combining the above challenges: We utilize a new[45] well-characterized system consisting of planar neutral nanoparticles with grafted alkyl chains; these colloids are suspended in two different solvent media in an effort to explore different possibilities for tuning gelation and phase separation. The nanoparticles are schematically shown in Fig. 1 and have a characteristic size of about 1.5 nm. Gelation was observed in both homogeneous one-phase and heterogeneous phase-separated suspensions of the same particles in toluene and decane at different volume fractions. Common in both cases is cluster formation and subsequent structural arrest, whereas the thermodynamic phase coexistence and the sol–gel transition lines exhibit a distinct dependence on the solvent used. More specifically, for the suspension of the grafted organosilicate particles in toluene, the gel line lies above the phase separation line, hence it inhibits phase separation. On the other hand, for the suspension in decane, the gel line intersects the phase coexistence boundary, hence it arrests phase separation. In both cases, gelation is observed at relatively high concentrations, suggesting short-range attraction in these systems. This argument is further supported by the estimated short length of the grafted chains (less than 0.8 nm) which relates to the range of attraction (the latter being smaller) as is for example discussed in the Baxter adhesive hard-sphere potential.[46,47] Moreover, comparing the two systems, one can note that whereas both solvents are bad for the organosilicate, decane is better solvent for the grafted alkyl chains compared to toluene. It does penetrate the chemically identical swollen alkyl chains and in such a crowded environment it crystallizes.[38] Crystallization of nearly aligned crowded alkyl chains is a common phenomenon.[48] Here, it results in grafted particles with a crystalline coat that acts as a strong attraction site, and hence gelation in the decane suspension occurs at lower concentrations compared to its toluene counterpart at room temperature.

In the rest of this work, these two distinct cases of phase separation and gelation intervention will be discussed for grafted nanoparticles which alter their attractive interactions in the presence of different solvent for the grafted layer. The paper is organized as follows: In section II we present the materials and experimental techniques utilized. Then, the experimental results are presented and discussed in section III, and a tentative interpretation is offered in section IV. Finally, we summarize the main conclusions from this work in section V.

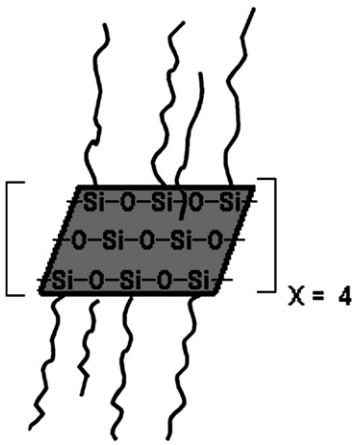

Fig. 1 Layered organosilicate hybrid with eight $C_{18}H_{37}$ alkyl chains.

II. Experimental

II.1 Materials

The layered organosilicate nanoparticles (LOS) were prepared as described previously.[45] Briefly, 4 g of octadecyltrichlorosilane (OTS, $C_{18}H_{37}SiCl_3$) were dissolved in 20 mL toluene, in a thoroughly pre-dried flask, to which H_2O (0.38 mL; H_2O/OTS = 2:1 molar ratio) was added. The mixture was refluxed for 24 h, whereupon a transparent dispersion was obtained. After completion of the reaction, methanol (40 mL) was added to the dispersion and the precipitate was copiously washed with methanol before drying at 70 °C. The crude product was dissolved in hot toluene (10 mL), followed by centrifugation to separate any insoluble products. After separation of the supernatant liquid, methanol (10 mL) was added and the precipitate was again isolated by centrifugation and dried at 70 °C. The resulting solid was ground into a powder, washed with acetone, and dried. The solid material melts into a transparent liquid above 55 °C. Homogeneous particle dispersions in toluene were readily obtained after gently stirring the nanoparticle/toluene mixture at low concentrations (<2 wt%) for few hours at 20 °C.

II.2 Techniques

A variety of experimental techniques were used in order to obtain unambiguous information on the phase and gel behavior of the

two experimental systems, LOS/toluene and LOS/decane suspensions. The experimental program consisted of measuring dynamics and structure at various concentrations and temperatures. The combined difficulty of limited sample (LOS) availability and limited resolution and/or applicability of techniques in different ranges (time, concentration, temperature) dictated the selection of techniques. More specifically, for both suspensions, above phase separation the suspensions were opaque and dynamic light scattering proved ideal to probe the evolution of the dynamics and the presence of clusters. In the gel state the samples were not transparent or even opaque, and rheology was employed to confirm the gelation. Turbidity was also used to detect phase coexistence, and pictures of selected samples in both the homogenous single-phase and phase-separated (or arrested) regions are included below. Finally, for selected samples in both solvents X-ray scattering (limited data) provided further support for the presence of clusters. As discussed below, this experimental program provides the necessary information to discuss the intriguing phenomena of solvent-mediated interplay of gelation and phase separation.

II.2.1 Photon correlation spectroscopy (PCS). In this dynamic light scattering experiment, the desired relaxation function $C(q,t) = \{[G(q,t)-1]/f^*\}^{1/2}$ was computed from the experimental autocorrelation function $G(q,t) = \langle I(q,0)\, I(q,t)\rangle / \langle I(q)\rangle^2$ of the polarized light scattering intensity $I(q)$ at a scattering vector $q = (4\pi n/\lambda_0)\sin(\theta/2)$ (n is the refractive index, θ denotes the scattering angle and λ_0 is the wavelength of the incident laser beam in vacuum); f^* is a coherence instrumental factor.[49] PCS measurements were performed for two LOS suspensions, in toluene and in n-decane. Previous experiments with similar clay systems confirmed the feasibility of the PCS to probe their dynamics.[50] Dust-free LOS suspensions were obtained by filtration of the dilute solutions in toluene and in n-decane through 0.2 μm Millipore filter at 20 °C and 35 °C, respectively. This method of preparation provided cluster-free well-dispersed particles.[51]

II.2.2 Small-angle X-ray scattering (SAXS). These measurements were carried out at the Synchrotron Radiation Source (SRS) in Daresbury Laboratory, Warrington, UK, on station 16.1. The sample–detector distance was 1.5 m and the wavelength was 1.41 Å. The samples were placed inside capillary tubes of 2 mm diameter, while a gas-filled area detector was used to collect data. Details concerning the station and the data collection electronics can be found elsewhere.[52] SAXS measurements were conducted with dense suspensions in n-decane in the gel state at 25 °C and sol state at 45 °C.

II.2.3 Shear rheometry. Rheological measurements were performed with a TA (formerly Rheometric Scientific) ARES-HR-100FRTN1 sensitive strain-controlled rheometer, using a Peltier element for temperature control (accuracy ±0.1 °C) and parallel plate (25 mm diameter) geometry. A home-made solvent trap system to maintain a saturated solvent atmosphere and reduce the risk of evaporation was occasionally used, although decane did not evaporate over measurement times of the order of 1 h at the test temperatures during this work. Dynamic frequency sweeps were carried out to probe the viscoelastic response of the test sample. These tests followed dynamic strain sweeps and time sweeps for establishing the conditions for linear viscoelastic response and steady state measurements, respectively. The protocol used consisted of the following steps: The sample was first heated to about 60 °C in the homogeneous region (at this temperature it was a Newtonian liquid) to erase any history (thermal, stress). Then, it was then into the rheometer fixture and the gap was gently adjusted. Subsequently, the temperature was set at 40 °C and the sample was equilibrated for 30 min before measuring. Different temperatures were reached in the same way, which ensured reproducibility of the measurements.

III. Results and discussion

III.1 Dilute regime

In the absence of interactions, the intermediate scattering (or relaxation) function $C(q,t)$ describes the decay of the concentration fluctuations due to mass diffusion,[49]

$$C(q,t) = \alpha \exp(-Dq^2 t) \quad (1)$$

with $\alpha \leq 1$ being the amplitude of $C(q,t)$ and D the nanoparticle translational diffusion.

Fig. 2 depicts the $C(q,t)$ for a dilute (0.9 wt%) LOS suspension in toluene at a constant value of the scattering wavevector $q = 6.14 \times 10^{-3}$ nm^{-1}. Note that toluene is a solvent of intermediate quality (between theta and good for the alkyl chains). The single exponential (solid line) decay with a diffusive rate $\Gamma = Dq^2$ (not shown) conforms to eqn (1), suggesting a rather low size polydispersity and a rather fast translational diffusion coefficient D ($\approx 2.5 \times 10^{-6}$ cm^2 s^{-1}), yielding a small average hydrodynamic size. The low scattering contrast α (≈ 0.05) is due to the weak scattering intensity of the diluted small particles. The absolute excess scattering intensity, $R_{vv} = \alpha I(q) R_{tol}/I_{tol}$ (I_{tol} and $R_{tol} = 2.78 \times 10^{-3}$ cm^{-1} being the scattering intensity and absolute Rayleigh ratio of the pure toluene at $\lambda_0 = 532$ nm, respectively)

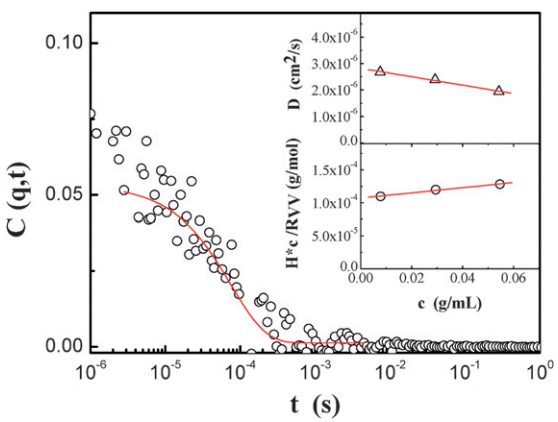

Fig. 2 The experimental relaxation function $C(q,t)$ for the concentration fluctuations in 0.9 wt% nanoparticles in toluene at $q = 6.14 \times 10^{-3}$ nm^{-1} (○) at 20 °C. The solid line denotes a single exponential behavior according to eqn (1). The extracted diffusion coefficient D (eqn (1)) and effective molar mass Hc/R_{vv} (eqn (2)) are depicted as a function of the concentration, c, in the two insets (top and bottom, respectively). The solid lines are linear fits to the experimental points.

was found to be q-independent, as expected for particles much smaller than the laser wavelength.[49,53] The linear variation of inverse reduced intensity c/R_{vv} in the lower inset of Fig.2 is represented by:

$$cH/R_{vv} = 1/M_w + 2A_2c \quad (2)$$

where $H = (2\pi n\, dn/dc)^2/(\lambda_0^4 N_A)$ is the optical constant of the suspension with N_A being the Avogadro number. The refractive index increment dn/dc ($= 0.034$ cm^3 g^{-1}) was measured at $\lambda_0 =$ 633 nm using a scanning Michelson interferometer[54] (at the Max-Planck Institute for Polymer Research, Mainz, Germany). The linear fit of eqn (2) to the data yields the molar mass $M_w = 9.4 \pm 0.5$ kg mol^{-1} and the second virial coefficient $A_2 = 2 \times 10^{-4}$ cm^3 mol g^{-1}. The positive, albeit small, value of the latter (in toluene at 20 °C) signifies good solvent conditions, whereas its low value should not affect the concentration dependence of the translational diffusivity. Indeed, D (upper inset to Fig. 2) conforms to the linear concentration dependence:

$$D = D_0\,(1 + k_D c) \quad (3)$$

D decreases weakly with c, with the coefficient $k_D = -5.6$ cm^3 g^{-1}, which reflects the kinetic effect of the friction coefficient on D. Under the assumption of nearly spherical particles, the single particle diffusivity from the Stokes–Einstein–Sutherland relationship[1] $D_0 = k_B T/(6\pi\eta R_h)$, with η being the solvent viscosity and k_B the Boltzmann constant, yields the effective hydrodynamic radius $R_h = 1.4 \pm 0.1$ nm of the LOS particles. Therefore, these nanoscopic hairy particles grafted with about thirty-two $C_{18}H_{37}$ chains exhibit typical good solvent behavior in dilute solution in toluene. The estimated overlapping volume fraction is $\phi^* \sim 3M_w/(4\pi R_h^3 N_A \rho)$, ρ being the particle density, and approaches the melt volume fraction ($\phi \sim 1$). The effect of non-spherical shape of the OTS particles is to reduce this value due to the large required rotational volume[51] and hence narrow the dilute regime. For our purposes here there is no need to account for the asphericity.

III.2 Thermoreversible gelation and phase separation.

III.2.1 Gelation in the one-phase region: LOS in toluene. The nanoparticle suspension remains a low-viscosity fluid at 20 °C up to a concentration of about 28 wt% in toluene. At and above this concentration, the experimental $C(q,t)$ does not relax within the experimental time window of PCS, as seen in Fig. 3. At the same time, it can be observed that the transparent suspension becomes more viscous than the solvent. Therefore, as already reported in other systems, the intermediate scattering function serves as a sensitive indicator of the arrest of the concentration fluctuations and hence the onset of non-ergodic behavior in the system due to static inhomogeneities.[10,14,25,26,55–58] On the other hand, at the same concentration ergodicity is immediately restored upon heating the suspension to 28 °C; this is clearly evidenced by the full decay of $C(q,t)$ in the experimental time window (not shown). However, $C(q,t)$ exhibits now a two-step relaxation (as can be clearly observed in Fig. 3 for 35 °C), associated with the fast particle diffusion and the slow diffusive motion which is

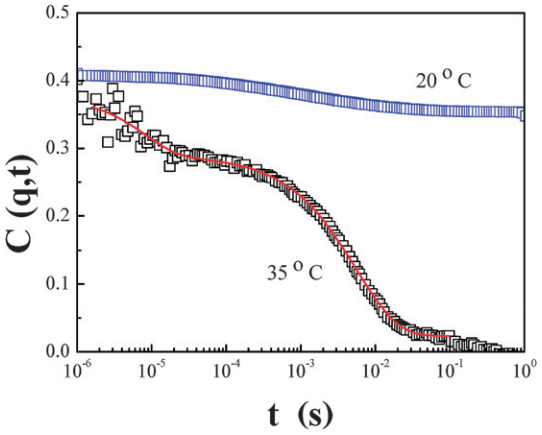

Fig. 3 The intermediate scattering function $C(q,t)$ for the concentration fluctuations for a 32.8 wt% LOS nanoparticle/toluene suspension at two temperatures, 35 °C ($q = 0.018$ nm^{-1}) with ergodic behaviour, and 20 °C ($q = 0.034$ nm^{-1}) with non-ergodic behaviour.

attributed to clusters. The enhanced low-q scattering intensity and the evolution of the slow mode in PCS, which becomes stronger in intensity and slower in time and eventually gives rise to non-ergodicity, are strong indications of cluster formation.[10,11,50,51,53] Moreover, results from systematic measurements at different concentrations suggest that the cluster population progressively increases above a concentration of 5 wt%. In fact, it is this slow relaxation process that freezes at 20 °C and gives rise to the non-ergodic plateau in $C(q,t)$, seen in Fig. 3. It appears, therefore, that the cluster formation relates with the kinetic arrest of the nanoparticle suspension.[17,30,59–64] For the 28 wt% LOS/toluene suspension at hand, this kinetic frustration (which we shall call gelation) occurs at $T_{gel} = 28$ °C. T_{gel}, determined at different nanoparticle concentrations in the range 28–60 wt%, is mapped into the phase-state diagram of Fig. 4. Our data suggest that 28 wt% corresponds to a critical gel,[65] namely the onset of percolation (in fact in the region 28–30 wt% we find rheologically critical gel behavior, as discussed below). Whereas below this concentration the dynamics are slowed, the cluster relaxation time does not diverge since the clusters do not percolate. The system can thus reach equilibrium over experimental time scales and phase separate. Note in this figure that above about 60 wt% in LOS, the phase boundary reflects the liquid–solid phase coexistence, manifesting the much stronger concentration dependence of the melting point of the dense nanoparticle suspension. Alternatively, small amounts of solvent added to the solid LOS particles ($c = 100$ wt%) act as effective plasticizers, reducing the melting point. A final remark relates to the possible link between the gel line and the gas–solid phase line. Since we do not have sufficient evidence to confirm this, we decided not to connect the gel and liquid–solid lines in Fig. 4. On the other hand, we note that the short range of the attractions supports the possibility of such a link. It is certainly intriguing that gelation could possibly follow this phase envelope.[46,66]

One possible origin of the observed gelation behavior of the nanoparticle suspension at relatively high concentration but rather low apparent (based on an average estimated hydrodynamic size) volume fraction of $\phi = (cN_A/M_w)(4\pi R_h^3/3) = 0.2$ is the thermodynamic incompatibility, usually proposed for

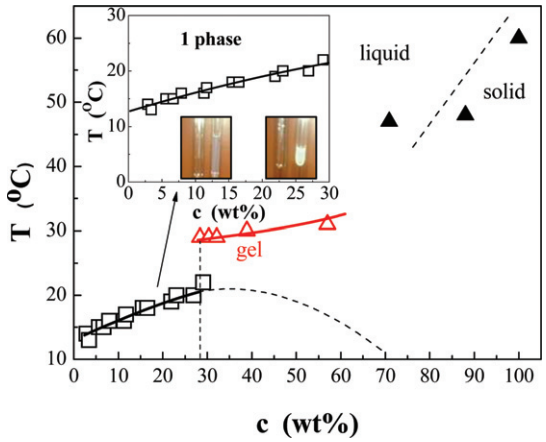

Fig. 4 Phase and state behaviour of the LOS nanoparticle suspension in toluene. The sol-gel temperature (T_{gel}) and the melting point (T_m) are indicated by open and solid triangles, respectively. The vertical dashed line indicates the critical gel concentration (28 wt%). The lines through the gel and solid–liquid data are to guide the eye. Likewise, the line through the coexistence data (open squares) serves as guide to the eye (see text for possible connection). Whereas the solid part indicates measured data, the dotted line is drawn simply as a continuation of the measured binodal curve. In this region we cannot determine the binodal since gelation occurs at higher temperatures and the suspensions in this regime cannot equilibrate. The arrow indicates the inset which contains details of the measured binodal. Inset: The phase coexistence point of the liquid suspension in the range 0–30 wt% with two photographs of the clear (left) and phase separated (right) suspension at low (7.5 wt%) at high (30 wt%) concentrations. The solid lines are to guide the eye.

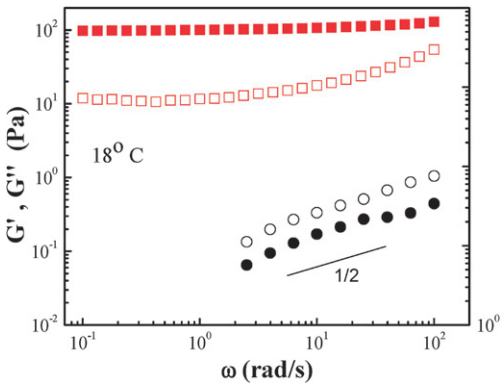

Fig. 5 Frequency-dependent linear viscoelastic moduli in LOS/toluene suspension at $T = 18$ °C and LOS concentrations $c = 30.1$ wt% (circles) and about 58 wt% (squares). Solid symbols represent storage modulus G' and open symbols are for loss modulus G''.

polymer nanocomposites,[67] which should lead to some kind of attraction. In spite of the small but positive A_2 (eqn (2)), at low concentrations at 20 °C, the suspension becomes weakly opaque below about 15 °C, as seen in the left picture in the inset of Fig. 4. This particle–solvent phase separation becomes apparent at higher concentrations $c \geq 28$ wt% (right picture in inset of Fig. 4, for $c = 30$ wt%). The binodal phase boundary for liquid–liquid coexistence in this concentration region lies at temperatures lower than T_{gel}, as shown in Fig. 4. Note that for concentrations larger than 28% we cannot determine the binodal since gelation occurs at higher temperatures and hence the system is out-of-equilibrium. We thus draw the dotted part of the binodal simply as a continuation of the part that we do measure.

Particle clustering is already evident in the experimental $C(q,t)$ at concentrations lower than 28 wt% (appearance of slow mode), assisted by the increasingly unfavorable interactions due to the proximity to the liquid–liquid phase coexistence. However, cluster formation does not necessarily imply macroscopic gelation, unless the dynamic response is simultaneously arrested (Fig. 3). We assign gelation to the experimental state where the concentration fluctuations become slower than the experiment time and non-ergodicity develops (see for example, Fig. 3 at 20 °C). Although below 28% LOS the dynamics are slowed, their lifetime does not diverge since the clusters do not percolate. The system can thus reach equilibrium over experimental time scales and phase-separate in this low-concentration region, hence we do not expect the gel line to meet the binodal in Fig. 4. These two lines have very different origins: the binodal is an equilibrium thermodynamic feature, whereas the gel line reflects a dynamic arrest.

Additional experimental evidence comes from rheological measurements. Fig. 5 depicts the linear viscoelastic spectrum (frequency-dependent storage (G') and loss (G'') moduli) for a LOS suspension in toluene at $c = 30.1$ wt% and $T = 18$ °C. Over nearly 2 decades in frequency the moduli are parallel with a slope of about ½ with respect to frequency and with G'' slightly exceeding G'. This is a signature of a correlated system relaxing in a self-similar manner as a weak gel. This kind of behavior has been observed in other colloidal systems such as block copolymer micelles and multiarm star polymers, and assigned to transient gel formation as a precursor to the glassy state at larger volume fractions.[68,69] It can be thought of as a critical gel state,[65] *i.e.* the onset of cluster percolation in the present system. For the purpose of the present discussion, the rheological signature is consistent with the dynamic light scattering data. It is interesting to note, however, that the measured viscosity appears to explode throughout the percolation transition. Indeed, from the limited data at 28 wt% and different temperatures, the viscosity increases by at least an order of magnitude from 40 °C (1.5 mPa s) to 18 °C (larger than 20 mPa s since no Newtonian plateau is detected). Similarly, for particle concentrations below 28 wt%, the suspension remains a low-viscosity liquid irrespective of the temperature, down to the lowest examined temperature of 15 °C. The barely resolved Newtonian viscosity is about that of water (1 mPa s), exhibiting the same weak temperature dependence. We also show in Fig. 5 that linear response data for a suspension well into the gel region (about 58 wt% at the same temperature of 18 °C). Indeed, a typical rheological signature of a strong gel is observed, *i.e.* G' being frequency-independent and clearly larger than the weakly frequency-dependent G'' over 3 decades in frequency. The corresponding (apparent) viscosity at the lowest measured frequency exceeds 10^3 Pa s.

The phase behavior depicted in Fig. 4 is qualitatively similar to the simulated phase diagram of physically associating polymer solutions *via* introduction of "stickers" on the chain backbone[30] and of particles interacting *via* a square-well potential supplemented by a constraint on the maximum number of bonded

interactions. Both the phase boundary, where the solution separates in polymer-rich and particle-rich phases, and the gel line $T_{gel}(c)$ where the chain diffusivity approaches zero, vary weakly with concentration. It appears that the transient localization of the nanoparticles forming the clusters should lead to sufficiently slow dynamics and eventually non-ergodicity and gelation. It should be noted, however, that this particular situation appears to contradict the recent suggestion that phase separation necessarily triggers gelation in short-range attractive colloids.[23,24,60,70] Of course, that suggestion was based on three qualifications, namely no gravity effects, spherosymmetric interactions and short-range attractions. The present experimental system appears to fulfil these qualifications: over the course of several months, no evidence of sedimentation was found. Despite insufficient evidence to argue for truly spherosymmetric interactions, it is clear that they are not anisotropic for these grafted planar nanoparticles (no evidence of induced anisotropic structures based on DLS). Lastly, the observation of gelation at high concentrations suggests short-range attraction. This is further supported by the estimated length of the grafted chains (about 0.8 nm) as already discussed. True enough, the present system consists of particles, tethered chains and solvent, with complicated interactions compared to the model colloid/polymer mixtures. The LOS/toluene system bears similarities with generic situations where kinetic arrest (here controlled by particle bonding[30]) inhibits the phase separation.[71]

III.2.2 Gelation in the two-phase region: LOS in decane. Based on the above findings, it appears that tuning the state of the nanoparticle suspension, and in particular T_{gel}, should be feasible by varying the solvent quality. To test this possibility, we investigated the suspension of LOS in decane, which is a good solvent for the hydrocarbon-grafted chains. Unexpectedly, this system was found to undergo the phase separation at higher temperature (about 32 °C) than for the LOS/toluene suspensions. The interactions of the swollen hydrocarbon ligands with decane appear to be at the origin of the changed particle interactions in the former case. In fact, the hydrodynamic radius of LOS in dilute suspensions in decane is larger than in toluene ($R_h = 2.8$ nm at 45 °C). Decane molecules would penetrate (or intercalate) the brush formed by the grafted chains and depending on temperature they may mix randomly with the alkyl chains or order into intermolecular crystalline packings.[38] At high concentrations above about 11 wt%, clusters dominate the experimental $C(q,t)$ of the LOS/decane system shown in Fig. 6 (for $c = 17.8$ wt%), as becomes evident from its slow dynamics and high contrast (*cf.* Figs. 2 and 3). Note that the fast diffusion process seen in Fig. 3 for the LOS/toluene system is hardly discernible in Fig. 6 (in the range of 10^{-4} s). In the single-phase region (at 38 °C), the relaxation function $C(q,t)$ of the 26.6 wt% nanoparticle suspension fully relaxes within the experimental time window of the PCS technique, and the fluid suspension remains ergodic up to the phase separation temperature. The latter was estimated from the experimental light scattering intensity $I(T)$ which diverges at the spinodal temperature (26 °C) obtained from the linear part of I^{-1} *vs.* T^{-1} (inset to Fig. 6). In contrast to the LOS/toluene system, the LOS/decane suspensions remain liquid in the one-phase region well above and near the phase boundary, and a possible gelation transition occurs in the

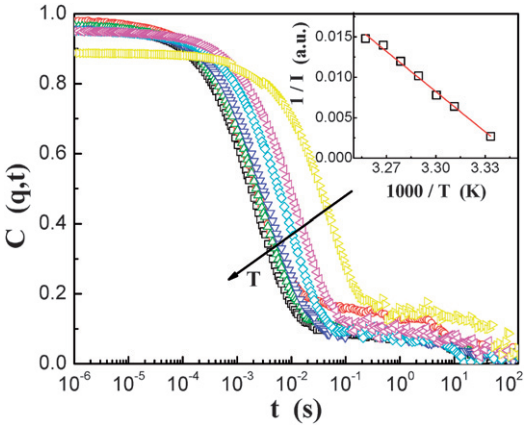

Fig. 6 The intermediate scattering function $C(q,t)$ of the 17.8 wt% LOS/decane suspension at $q = 0.0235$ nm^{-1} and different temperatures increasing in the direction of the arrow from 27 °C to 34 °C. The arrow indicates increasing temperatures from right: 27, 29, 30, 31, 32, 33 and 34 °C. Inset: The strong increase of the light scattering intensity (I) with decreasing temperature towards phase separation (at 26 °C) is shown in the plot $1/I$ *vs.* $1/T$. The line denotes the fit to the mean field expression with the spinodal temperature at 26 °C.

two-phase region. In other words, it appears that in the latter system the gel line crosses the phase boundary.[60]

The phase diagram of the LOS/decane suspension was obtained from a combination of PCS and turbidity measurements which yield the binodal temperature presented in Fig. 7 as a function of the particle concentration. Up to a concentration of about 11 wt% (apparent volume fraction of $\phi \approx 0.08$), thermodynamic equilibrium is warranted and the phase separation is characterized by a transparent solvent-rich upper phase and an opaque nanoparticle-rich lower phase, as shown by the image in the left corner of Fig. 7. Up to this volume fraction phase separation does not trigger kinetic arrest. This, however, appears to occur at higher concentrations, as seen in Fig. 7, due to the

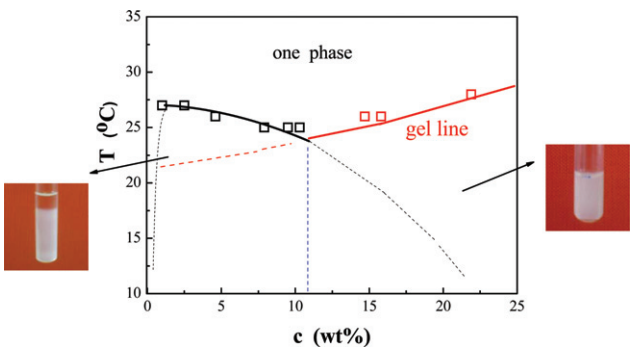

Fig. 7 Phase behavior of the nanoparticle suspension in decane obtained by PCS and turbidity measurements. For concentrations above about 11 wt% (vertical dashed line) a clear phase separation into solvent-rich and nanoparticle-rich phases is kinetically prohibited, as seen by the two photographs in the insets (the left shows two phases, top clear and bottom opaque; the right shows a frozen opaque single state). The thick solid and thin dashed lines are to guide the eye. The former indicate measured boundaries whereas the latter are drawn schematically as continuations.

intervention of the gel line (see also the image in the right corner of Fig. 7);[23,24,60,70] hence, gelation here appears as an arrested phase separation, as discussed in the context of short-range attractive colloids.[23,24,60] The latter effect is also reminiscent of the interplay of glass transition with phase separation in polymeric binary mixtures.[71,72] It is worth noting that the arrested state occurs at significantly lower nanoparticle concentrations compared to the toluene suspensions (Fig. 4), but at similar solidification temperatures (around 30 °C). The sample's appearance (image in the right corner of Fig. 7) remained unchanged over a period of two months.

To gain more insight into the local structure of concentrated LOS/decane suspensions, we performed SAXS measurements of a 22.5 wt% concentration at two temperatures, in the homogeneous liquid phase (at 45 °C) and the opaque gel-like state (at 25 °C). The obtained SAXS patterns are depicted in Fig.8. In the low-viscosity liquid phase at 45 °C, the broad peak centered at $q_1^* \approx 1.5$ nm^{-1} suggests a weak liquid-like ordering with an average spacing between the nanoparticles of $d = 2\pi/q_1^* \approx 4$ nm, anticipated from their number concentration, *i.e.* $d \approx (cN_A/M_w)^{-1/3}$. In contrast, the gel-like state of the same suspension at 25 °C displays a richer structure. The presence of a narrower and very intense peak at $q^* \sim 0.7$ nm^{-1}, accompanied by two weak higher-order peaks at about $2q^*$ and $3q^*$, suggests a layered structure. This pronounced ordering corresponds to an interlayer spacing of about 9 nm, which is larger than the reported spacing of about 6 nm in the solid material ascribed to stacks of bilayers.[45] Here, the swelling by the solvent decane and intermolecular ordering of decane and grafted $C_{18}H_{37}$ chains into packings

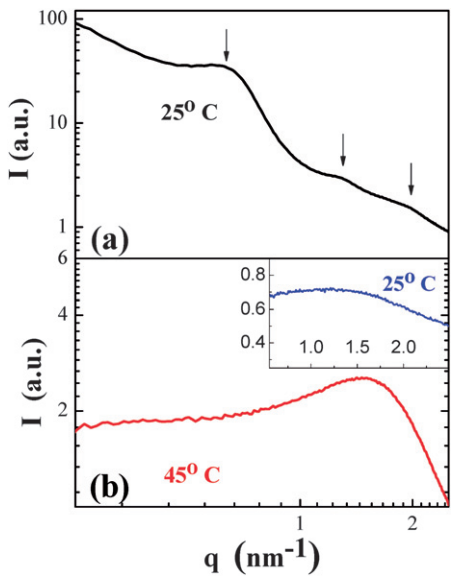

Fig. 8 SAXS patterns of the nanoparticle LOS/decane suspension at 22.5 wt% in the opaque gel (a, 25 °C) and the clear liquid (b, 45 °C) states, below and above the phase separation temperature, respectively. The vertical arrows in (a) indicate the main peak position q^* (left) and the weaker and broader secondary ones $2q^*$ and $3q^*$, which are typical of liquid-like arrangement of the particles. No evidence of macrocrystalline arrangement is found. Inset to (b): Respective profile of the LOS/toluene suspension at 4.5 wt% and 25 °C, in the clear liquid state (same axes labels as a and b). The weak, broad peak is suggestive of liquid-like order.

of alkane crystals[38,73] can rationalize the larger spacing in the nanoparticle suspension and hence the shift of the SAXS peak of the gel-like microphase separated nanoparticles to low q values. The concurrent opaque appearance of the nanoparticle suspension (right image in Fig. 7) due to clusters is also evident by the further increase of the SAXS intensity at low q. Therefore, the SAXS profile of Fig. 8 at 25 °C implies the presence of clusters with an internal layered structure. The increased coherence of this structure, as evidenced by the narrow width of the main peak and the presence of higher-order SAXS peaks at 25 °C, leads to the slowing-down of the dynamics, a prerequisite for a frustrated macrophase separation. The occurrence of gelation at lower concentrations than for the suspensions in toluene suggests an increased van der Waals attraction between particles with the internal alkyl crystalline packing.

In view of the experimental program outlined in section II above, a remark is in order. We performed selected SAXS measurements with the LOS/toluene suspension at 25 °C (inset to Fig. 8b). Typically, for a 4.5 wt% suspension the intensity profile consists of a broad and weak low-q peak, which is suggestive of possible interactions but does not constitute evidence of cluster formation (from PCS interactions and clustering are clearly evident above 5 wt%). In fact, it is suggestive of liquid-like arrangement in this system with an average spacing between the nanoparticles of about 5.5 nm. This spacing is in agreement with the corresponding spacing (4 nm, Fig. 8b) in LOS/decane at 45 °C considering its larger hydrodynamic size (2.8 nm). Since the LOS/toluene system undergoes the liquid–gel transition in the homogeneous one-phase region, there is no SAXS experiment in the two-phase region corresponding to LOS/decane analogue in Fig. 8a. Overall, the SAXS data are consistent with the picture emerging from Figs. 4 and 7. Note that, whereas further analysis of cluster morphology is in principle possible with sophisticated approaches accounting for non-ergodicity (for example multi-speckle scattering),[10,11] this is an interesting dedicated study that could complement this work in the future.

To further elucidate the nature of the solidified nanoparticle suspension (for $c > 11$ wt%), the linear viscoelastic response of a 21.6 wt% ($\phi \approx 0.22$) sample was probed. At 40 °C, with the sample being transparent, the dynamic frequency sweeps were performed at the limit of the rheometer's torque resolution, but nevertheless revealed an unambiguous (and consistent with the sample's appearance) Newtonian liquid behavior, where over about one decade in frequency $G'' > G'$; G'' displayed the expected frequency scaling ($\sim\omega$), whereas G' (not well-resolved) barely obeyed the ω^2 scaling rule. Upon subsequent quenching to 20 °C, the sample became opaque. A dynamic time sweep at a frequency of 1 rad s^{-1} and strain amplitude of 1% indicated that after about 30 min the sample was not fully equilibrated (Fig. 9), suggesting slow transformation (gelation) kinetics. However, as our purpose was to probe the sample's state and not to investigate the time evolution of the gel in detail, we did perform a dynamic frequency sweep after about 45 min. As seen in Fig. 9, the sample exhibited a clear solid-like response. Note that the apparent slight enhancement of G' at the lowest frequencies is an indication of the still-evolving modulus (kinetics). Therefore, despite the barely quasi-equilibrium nature of these measurements, the solid-like character of the sample at 20 °C is unambiguously demonstrated. Finally, after the measurements were

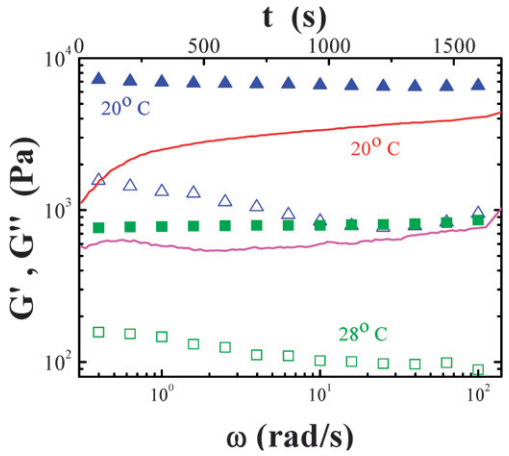

Fig. 9 Frequency-dependent storage (G' solid symbols) and loss (G'' open symbols) moduli of the 21.6 wt% nanoparticle LOS/decane suspension, measured under two protocols: (i) at 20 °C after quenching from 40 °C and 45min equilibration time (triangles), and (ii) at 28 °C after heating from 20 °C (squares). The time evolution of the moduli before the dynamic frequency sweeps in the former case (i) is also shown (G' (upper line), G''(lower line)).

completed at 20 °C, we heated-up the sample to 28 °C, and after a waiting period of about 10 min, we performed a dynamic frequency sweep. As evidenced from Fig. 9, the sample remained a viscoelastic solid, with reduced moduli (compared to the 20 °C case) by more than a decade.

IV. Rationalization: tuning the interplay of gelation and phase separation

It is evident from the above results that the LOS suspensions in toluene (section III.1) and in decane (section III.2) behave quite differently in many ways: (i) The suspensions in toluene appear to gel for particle concentrations greater than 28 wt% (apparent $\phi \approx 0.2$). They phase-separate at lower temperatures compared to the gelation temperatures, and so the gel line prevents phase separation. (ii) The behavior of the LOS suspensions in decane indicates that gelation occurs for lower concentrations (as low as 11 wt%, or apparent $\phi \approx 0.08$). Gelation here may occur inside the two-phase region of the phase diagram for the particle/solvent system. The gel line intersects the phase coexistence line and arrests phase separation. Both gelation and phase separation temperatures are higher compared to the toluene case.

Our current understanding of the behavior of the decane system is motivated by earlier work by Grant and Russel[41] who investigated the behavior of silica colloids grafted with hydrocarbon chains and suspended in hexadecane, a good solvent for the chains. By varying the temperature it was found that the effective particle–particle interaction was attractive, and consequently the particles formed gels, with this gel formation occurring in the vicinity of phase separation. Similar studies by Verduin and Dhont[46] on silica particles coated with stearyl alcohol dispersed in benzene provide additional supporting evidence. Recent elegant work on the conformation of the grafted chains in the presence of a good, chemically similar solvent (hydrocarbons) using surface-specific vibrational spectroscopy[38,73] revealed that the solvent mixes entropically with the grafted chains at high temperatures but tends to order into crystalline packings of the alkanes as the temperature is lowered. These packings form an effective boundary layer around the particle (a kind of crystalline coat around the LOS particle) and lead to increased van der Waals attraction, hence gelation. Therefore, whereas decane is better solvent for the alkyl-grafted chains which are more swollen compared to toluene, it appears to mediate increased attractions. Clearly, the crystalline coat makes the attractions long-ranged compared to toluene. Moreover, recent theoretical work[30] for chains with a small fraction of stickers found precisely the same phenomenology as in the current experiments in decane and the experiments of Grant and Russel.[41] In the simulations, the attractive interactions between the stickers yielded both phase equilibrium and a gel. In most cases, gelation would thus manifest itself as an arrested phase separation, exactly as observed experimentally here. The major point to be stressed here is that gelation in these cases is driven by attractions between the particles forming clusters already in reasonably dilute conditions (section III.2). At concentrations above about 11 wt%, particle clustering becomes extensive (Fig. 7) and phase separation will eventually be arrested due to the intervention of the gel line. As mentioned already, analogous findings on the interplay between phase coexistence and gel or glass lines have been reported in the literature for polymeric mixtures.[71,72]

One may then expect an effect of the solvent molecular size on the phase coexistence. We have verified this conjecture in LOS suspensions by using two polymeric solvents, 1,4-polybutadiene with relatively low molar masses of 1 kg mol^{-1} and 4 kg mol^{-1}, respectively. One can observe in Fig. 10 that the phase separation is shifted to higher temperatures, as the molecular size of the solvent increases. Moreover, the gelation documented by shear rheometry takes place in the two-phase region and progressively at lower concentration as the molar mass of the solvent increases. Note that in the case of hydrocarbon solvents, opaque gels were always obtained.

The account of the situation in toluene we need to account for the fact that gelation appears to occur only in the one-phase region and at higher LOS concentrations. In the LOS/toluene

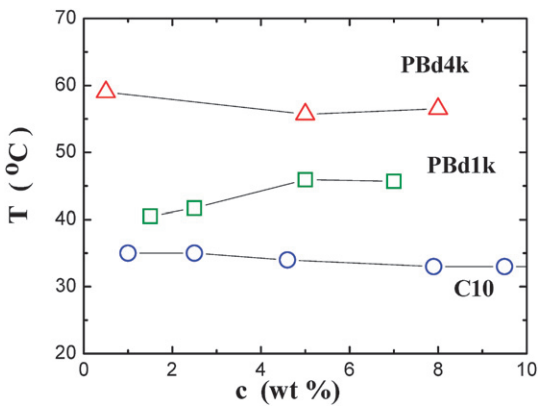

Fig. 10 Phase diagram of the nanoparticle suspension in polymeric solvents (polybutadienes PBd1k and PBd4k with molar masses of 1 kg/mol and 4 kg/mol, respectively) and decane (C10) obtained by rheological and turbidity measurements.

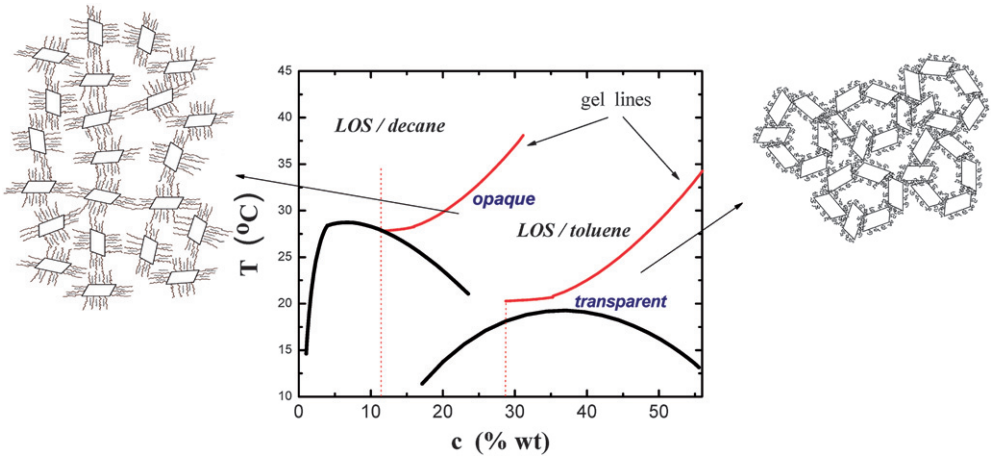

Fig. 11 Schematic drawing of the phase behavior of the LOS nanoparticle (Fig. 1) suspensions in the two solvents. In toluene transparent gels are formed at high concentrations before phase separation (right cartoon) whereas in decane the gel line traverses the phase diagram leading to non-transparent gels (clusters with internal crystallinity). Note that the cartoons are not drawn to scale with respect to the grafted chains: In toluene the grafted chains are less swollen. In decane the chains are swollen and with the enhanced penetration of solvent they form the attractive crystalline coat. Grafted particle interpenetration is also possible.

suspensions, the small but positive second virial coefficient at 20 °C (eqn (2) and inset of Fig. 2) is consistent with the virtual absence of clustering at low concentrations; however, it also implies solvent conditions that do not favor demixing. We note that the lowest binodal temperature is about 15 °C, less than 10 °C above the melting point of the neat toluene; this proximity might have an impact upon the solvent quality at temperatures below 20 °C. A persuasive picture is based still on attractive interactions between the LOS particles, in qualitative analogy to the LOS/decane system, *i.e.* a short-range attraction and a repulsion (coat) at longer ranges. But in the toluene case the grafted layer is not as swollen and not packed into a crystalline arrangement (reduced solvent quality compared to decane) and the attractive forces are short-ranged (larger gelation concentrations). The kinetic arrest that causes gelation is associated with the formation of cluster structures which eventually percolate and reduce the driving force for phase separation. This route to the thermoreversible gel state in the present LOS/toluene system is again consistent with the Grant–Russel analysis[41] and further supported by a recent numerical study for a system of particles with attractive particle–particle interactions which, however, are switched-off when one of the two interacting particles has a pre-selected aggregation number (≤12).[60] Based on the above discussion, it seems that the weaker particle attractions in the LOS/toluene system relate to transparent gels.

V. Concluding remarks

In this work we have presented two solvent-mediated pathways to the gelation of grafted nanoparticle suspensions. For the organosilicate systems grafted with alkane chains, when the solvent is toluene (which is a good solvent for the grafted chains and a rather bad solvent for the bare particles), a gel state is formed at high concentrations in the homogeneous region, and the phase separation occurs (where kinetically possible) at temperatures below the gel line. On the other hand, when the solvent is decane (which is a better solvent for the grafted chains but a bad – and in fact even the worst solvent – for the bare particles), gelation takes place at much lower concentrations, in the vicinity of the phase boundary. The key factor here is the formation of a crystalline coat around the nanoparticle due to the solvent that penetrates the swollen grafted chain layer. The common feature of the observed behavior in both cases is the cluster formation (*via* attraction of different strength and range) and the subsequent dynamic arrest. The interplay of gelation and phase separation in these systems is illustrated schematically in Fig. 11 and shows the possibilities for tailoring the state of the suspension by appropriate choice of the solvent. An important remark is that gelation is not necessarily triggered by phase separation. This is in agreement with the general picture of interplay of kinetic arrest and phase separation in other classes of soft matter,[71,72] and in contrast to recent suggestions for (simpler) attractive colloidal systems,[23,24] thus providing alternative routes for the connection between gelation and phase separation in short-range attractive colloidal systems.[74,75]

Based on the obtained experimental evidence, the phase states of this system can be shifted in the $T(c)$ plane mainly by solvent–particle thermodynamic interactions but also thermodynamic transitions, *e.g.*, crystallization (LOS/decane). The presence of phase separation in the intermediate vicinity of the gel line as seen in Fig. 11 corroborates the notion of particle–particle attraction in both systems. In the case of LOS suspensions in decane, gelation is driven by a solvent-mediated stronger particle–particle attraction and occurs inside the two-phase region which is typical for short-range attractive colloid/polymer mixtures.[23,24] The apparent different phase behavior of LOS suspensions in toluene is rationalized by the weaker shorter-range attractive interactions.

Acknowledgements

We would like to thank B. Mueller and E. Pavlopoulou for the refractive index contrast and the SAXS measurements, respectively, as well as A. Larsen and D. Kendristaki for assistance in

some PCS and rheology measurements. We are grateful to B. Loppinet for helpful discussions and to J. K. G. Dhont for insightful comments and for bringing to our attention refs. 38 and 73. This work was supported in part by the EU NoE-Softcomp (NMP3-CT-2004-502235). EPG acknowledges the support of Award No. KUS-C1-018-02, made by King Abdullah University of Science and Technology (KAUST).

References

1 W. B. Russel, D. A. Saville and W. R. Schowalter, *Colloidal dispersions*, Cambridge University Press, NY, 1989.
2 P. N. Pusey, *Colloidal Suspensions in Liquids, Freezing and the Glass Transition*, ed. J.-P. Hansen, D. Levesque and J. Zinn-Justin, Elsevier, Amsterdam, 1991.
3 M. E. Cates and M. R. Evans, *Soft and Fragile Matter: Nonequilibrium Dynamics, Metastability and Flow*, Institute of Physics Publishing, Bristol, 2000.
4 H. Hoekstra, J. Mewis, T. Narayanan and J. Vermant, *Langmuir*, 2005, **21**, 11017.
5 J. Vermant and M. J. Solomon, *J. Phys.: Condens. Matter*, 2005, **17**, R187–R216.
6 S. C. Glotzer and M. J. Solomon, *Nat. Mater.*, 2007, **6**, 557.
7 J. M. McMullan and N. J. Wagner, *J. Rheol.*, 2009, **53**, 575–588.
8 F. Sciortino and P. Tartaglia, *Adv. Phys.*, 2005, **54**, 471.
9 K. A. Dawson, *Curr. Opin. Colloid Interface Sci.*, 2002, **7**, 218.
10 V. Trappe and P. Sandkuhler, *Curr. Opin. Colloid Interface Sci.*, 2004, **8**, 494.
11 L. Cipelletti and L. Ramos, *J. Phys.: Condens. Matter*, 2005, **17**, R253.
12 W. C. K. Poon, *Curr. Opin. Colloid Interface Sci.*, 1998, **3**, 593.
13 C. N. Likos, *Soft Matter*, 2006, **2**, 478.
14 E. Zaccarelli, *J. Phys.: Condens. Matter*, 2007, **19**, 323101.
15 F. Cardinaux, T. Gibaud, A. Stradner and P. Schurtenberger, *Phys. Rev. Lett.*, 2007, **99**, 118301.
16 S. K. Kumar and A. Z. Panagiotopoulos, *Phys. Rev. Lett.*, 1999, **82**, 5060.
17 S. Salaniwal, S. K. Kumar and J. F. Douglas, *Phys. Rev. Lett.*, 2002, **89**, 258301.
18 X. Zhang, Z. Wang, M. Muthukumar and C. C. Han, *Macromol. Rapid Commun.*, 2005, **26**, 1285.
19 H. N. W. Lekkerkerker, W. C. K. Poon, P. N. Pusey, A. Stroobants and P. B. Warren, *Europhys. Lett.*, 1992, **20**, 559.
20 D. Frenkel, H. N. W. Lekkerkerker and A. Stroobants, *Nature*, 1988, **332**, 822.
21 M. G. Basavaraj, G. G. Fuller, J. Fransaer and J. Vermant, *Langmuir*, 2006, **22**, 6605.
22 K. N. Pham, A. M. Puertas, J. Bergenholtz, S. U. Egelhaaf, A. Moussaid, P. N. Pusey, A. B. Shofield, M. E. Cates, M. Fuchs and W. C. K. Poon, *Science*, 2002, **296**, 104.
23 P. J. Lu, E. Zaccarelli, F. Ciulla, A. B. Schofield, F. Sciortino and D. A. Weitz, *Nature*, 2008, **453**, 499.
24 E. Zaccarelli, P. J. Lu, F. Ciulla, D. A. Weitz and F. Sciortino, *J. Phys.: Condens. Matter*, 2008, **20**, 494242.
25 D. Bonn, S. Tanase, B. Abou, H. Tanaka and J. Meunier, *Phys. Rev. Lett.*, 2002, **89**, 015701.
26 F. Ianni, R. Di Leonardo, S. Gentilini and G. Ruocco, *Phys. Rev. E*, 2008, **77**, 031406.
27 S. Cocard, J. F. Tassin and T. Nicolai, *J. Rheol.*, 2000, **44**, 585.
28 M. Rubinstein, R. H. Colby, *Polymer physics*, Oxford University Press, NY, 2003.
29 S. Obukhov, D. Kobzev, D. Perchak and M. Rubinstein, *J. Phys. I (France)*, 1997, **7**, 563.
30 S. Kumar and J. F. Douglas, *Phys. Rev. Lett.*, 2001, **87**, 188301.
31 M. P. Lettinga, K. Kang, A. Imhof, D. Derks and J. Dhont, *J. Phys.: Condens. Matter*, 2005, **17**, S3609.
32 M. Adams, Z. Dogic, S. L. Keller and S. Fraden, *Nature*, 1998, **393**, 349.
33 L. M. Liz-Marzán, *J. Mater. Chem.*, 2006, **16**, 3891.
34 J. Rodríguez-Fernández, J. Pérez-Juste, L. M. Liz-Marzán and P. R. Lang, *J. Phys. Chem. C*, 2007, **111**, 5020.
35 I. Pastoriza-Santos and L. M. Liz-Marzán, *Nano Lett.*, 2002, **2**, 903.
36 J. Mewis and J. Vermant, *Prog. Org. Coat.*, 2000, **40**, 111.
37 T. A. Witten and P. A. Pincus, *Macromolecules*, 1986, **19**, 2509.
38 S. Roke, O. Berg, J. Buitenhuis, A. van Blaaderen and M. Bonn, *Proc. Natl. Acad. Sci. U. S. A.*, 2006, **103**, 13310.
39 H. Verduin and J. K. G. Dhont, *J. Colloid Interface Sci.*, 1995, **172**, 425.
40 M. Chen and W. B. Russel, *J. Colloid Interface Sci.*, 1991, **141**, 564.
41 M. C. Grant and W. B. Russel, *Phys. Rev. E*, 1993, **47**, 2606.
42 J. Bergenholtz and M. Fuchs, *J. Phys.: Condens. Matter*, 1999, **11**, 10171.
43 C. G. de Kruif and J. A. Schouten, *J. Chem. Phys.*, 1990, **92**, 6098.
44 C. G. de Kruif, P. W. Rouw, W. J. Briels, M. H. G. Duits, A. Vrij and R. P. May, *Langmuir*, 1989, **5**, 422.
45 A. B. Bourlinos, S. R. Chowdhurry, D. D. Jiang, Y.-U. An, Q. Zhang, L. A. Archer and E. P. Giannelis, *Small*, 2005, **1**, 80.
46 H. Verduin and J. K. G. Dhont, *J. Colloid Interface Sci.*, 1995, **172**, 425.
47 P. W. Rouw and C. G. de Kruif, *J. Chem. Phys.*, 1988, **88**, 7799.
48 G. Petekidis, D. Vlassopoulos, G. Fytas, N. Kountourakis and S. Kumar, *Macromolecules*, 1997, **30**, 919.
49 R. Berne and R. Pecora, *Dynamic light scattering*, Wiley, NY, 1976.
50 D. Shah, G. Fytas, D. Vlassopoulos, J. Di, D. Sogah and E. P. Giannelis, *Langmuir*, 2005, **21**, 19.
51 D. Bonn, H. Kellay, H. Tanaka, G. Wegdam and J. Meunier, *Langmuir*, 1999, **15**, 7534.
52 N. Bliss, J. Bordas, B. D. Fell, N. W. Harris, W. I. Helsby, G. R. Mant, W. Smith and E. Towns-Andrews, *Rev. Sci. Instrum.*, 1995, **66**, 1311.
53 G. Fytas, Light Scattering from Dense Polymer Systems, in *Scattering Encyclopedia*, Academic Press, ed. P. Pike and P. Sabatier, 2002, vol. 1, (ch. 2.3.5), pp. 849–863.
54 A. Becker, W. Köhler and B. Müller, *Ber. Bunsen-Ges. Phys. Chem.*, 1995, **99**, 600.
55 F. Ikkai and M. Shibayama, *Phys. Rev. Lett.*, 1999, **82**, 4946.
56 M. Kapnistos, D. Vlassopoulos, G. Fytas, K. Mortensen, G. Fleischer and J. Roovers, *Phys. Rev. Lett.*, 2000, **85**, 4072.
57 V. A. Martinez, G. Bryant and W. van Megen, *Phys. Rev. Lett.*, 2008, **101**, 135702.
58 T. Eckert and E. Bartsch, *J. Phys.: Condens. Matter*, 2004, **16**, S4937.
59 A. Rissanou, D. Vlassopoulos and I. A. Bitsanis, *Phys. Rev. E*, 2005, **71**, 011402.
60 E. Zaccarelli, S. V. Buldyrev, E. La Nave, A. J. Moreno, I. Saika-Voivod, F. Sciortino and P. Tartaglia, *Phys. Rev. Lett.*, 2005, **94**, 218301.
61 F. Lo Verso, C. N. Likos, C. Mayer and L. Reatto, *Mol. Phys.*, 2006, **104**, 3523.
62 E. Del Gado and W. Kob, *Phys. Rev. Lett.*, 2007, **98**, 028303.
63 A. M. Puertas, M. Fuchs and M. E. Cates, *Phys. Rev. Lett.*, 2002, **88**, 098301.
64 Y.-L. Chen and K. S. Schweizer, *J. Chem. Phys.*, 2004, **120**, 7212.
65 H. H. Winter and M. Mours, *Adv. Polym. Sci.*, 1997, **134**, 165.
66 E. Lomba and N. G. Almarza, *J. Chem. Phys.*, 1994, **100**, 8367.
67 J. B. Hooper and K. S. Schweizer, *Macromolecules*, 2006, **39**, 5133.
68 F. Mallamace, S.-H. Chen, Y. Liu, L. Lobry and N. Micali, *Phys. A*, 1999, **266**, 123.
69 F. Ozon, G. Petekidis and D. Vlassopoulos, *Ind. Eng. Chem. Res.*, 2006, **45**, 6946.
70 A. Meller, T. Gisler, D. A. Weitz and J. Stavans, *Langmuir*, 1999, **15**, 1918.
71 G. Meier, D. Vlassopoulos and G. Fytas, *Europhys. Lett.*, 1995, **30**, 325.
72 K. Karatasos, G. Vlachos, D. Vlassopoulos, G. Fytas, G. Meier and A. DuChesne, *J. Chem. Phys.*, 1998, **108**, 5997.
73 S. Roke, J. Buitenhuis, J. van Miltenburg, M. Bonn and A. J. van Blaaderen, *J. Phys.: Condens. Matter*, 2005, **17**, S3469.
74 H. Takima, Y. Nishikawa and T. Koyama, *J. Phys.: Condens. Matter*, 2005, **17**, L143.
75 P. N. Pusey, A. D. Pirie and W. C. K. Poon, *Phys. A*, 1993, **201**, 322.